Delft University of Technology

Examining evaporative demand and water availability in recent past for sustainable agricultural water management in India at sub-basin scale

Singh, Vishal; Singh, Pushpendra Kumar; Jain, Sanjay Kumar; Jain, Sharad Kumar; Cudennec, Christophe; Hessels, Tim

Important note
To cite this publication, please use the final published version (if applicable).
Please check the document version above.

Examining evaporative demand and water availability in recent past for sustainable agricultural water management in India at sub-basin scale

Vishal Singh [a,*], Pushpendra Kumar Singh [a], Sanjay Kumar Jain [a], Sharad Kumar Jain [a,b], Christophe Cudennec [c], Tim Hessels [d]

[a] *Water Resources System Division, National Institute of Hydrology, Roorkee, 247667, Uttarakhand, India*
[b] *Department of Civil Engineering, Indian Institute of Technology, Roorkee, 247667, Uttarakhand, India*
[c] *UMR SAS, Institut Agro, INRAE, France*
[d] *Department of Water Management, Delft University of Technology, Delft, the Netherlands*

ARTICLE INFO

ABSTRACT

This study explores recent changes in evaporative demand and water availability across 100 river sub-basins in India by partitioning the actual evapotranspiration (AET) into green water evapotranspiration (ET-Green) and blue water evapotranspiration (ET-Blue). For computation of ET-Green and ET-Blue, the Budyko framework is applied to long-term scenario (2003–2017) and to intra-annual averaged series (i.e. 2003-2007, 2008–2012 and 2013–2017). For the Budyko analysis, the Climate Hazards Group InfraRed Precipitation with Station data (CHIRPS), Global Land Data Assimilation System (GLDAS) AET and Climate Research Unit Global Data Assimilation System (CRU GDAS) Potential ET (PET) climate forcing variables have been utilized. Multiple hydro-climatic indicators, such as dryness index (DI), evaporative index (EI), and responsivity with respect to theoretical Budyko curve are computed and they show substantial variations across sub-basins from far past time (2003) to recent past (2017). The changes in DI and EI highlight the diversity in evaporative demand and dryness condition across the country. Results reveal that India's evaporative water demand is largely influenced by ET-Green (up to 65%) that depends mainly on precipitation. At the same time, in many river sub-basins, ET-Blue that depends on external sources of water like diversion or stored water, is significant. The shape parameter (ω) of Fu's Budyko equation, that can be utilized for the future assessment of ET-Green and ET-Blue, has been optimized. The results of this study would of immense value for sustainable irrigation water management and improving water use efficiency in agriculture and overall water availability in river basins in India.

1. Introduction

The Budyko approach (Budyko et al, 1974), which can be defined by the semi-empirical expression, has been significantly utilized in many studies and it has emerged as one of the best methods of coupled water-energy balance (Li et al., 2019; Sposito, 2017). Budyko method mainly demonstrates the partitioning of precipitation into water yield/runoff (Q) and actual evapotranspiration (AET), which is influenced by the changes in precipitation and water demand i.e. potential evapotranspiration (PET) (Greve et al., 2015). Gunkel and Lange (2017) suggested that the available water (precipitation) and energy (radiation and temperature) can be considered for defining the regional hydro-climatic characteristics under the Budyko system. Budyko framework utilizes a well-known hydro-climatic scheme based on the evaporative index (EI) and dryness index (DI), which determines evaporative water demand and water stress conditions (or water scarcity) at larger scale in long-time durations, respectively (Simons et al., 2020). As per the Budyko theory, under no change conditions, the observation points (i.e. EI and DI corresponding to each sub-basin) should follow the theoretical Budyko curve (Creed et al., 2014). Any deviation of EI and DI from the theoretical Budyko curve suggest a change in the hydro-climatology of the river subbasin, one reason behind this could be climate change (Liu et al., 2019). Sinha et al. (2018) applied Budyko framework to assess the impact of climate variability and anthropogenic activities on hydrologic resilience in Peninsular India and found that many subbasins of the Southern India were not enough resilient.

Singh et al. (2021) and Simons et al. (2020) demonstrated that the irrigation water consumption (i.e. evaporative water demand) and

---

* Corresponding author.
E-mail address: vishal18.nihr@gov.in (V. Singh).

water availability can be effectively assessed through the quantification of total water in the form of green water and blue water in a basin. ET-Blue refers to the AET from the water stored in the groundwater or surface water (stored in rivers and lakes) which may be diverted to another river basin/subbasin to fulfill the AET demand (Simons et al., 2020). This can be achieved by partitioning the total AET into ET-Green and ET-Blue within the Budyko framework. Green versus blue water consumption in terms of ET-Green and ET-Blue fractions is mainly used to distinguish between consumption of precipitation versus groundwater and surface water (or stored water, viz. River, lakes, ponds etc.) (Singh et al., 2021; Simons et al., 2020).

Very few studies have utilized the Budyko framework for the assessment of variability related to the hydro-climatological changes of a region or any hydrological boundary impacted by changes in AET and PET (Li et al., 2019; Singh and Kumar, 2015). Many studies on climate change have shown that intensity and pattern of precipitation is changing in India (Singh and Kumar, 2019) and also around the world (Singh and Xiaosheng, 2019a, 2019b), and this has significantly affected AET, aggravating water shortages (Poonia et al., 2021; Huo et al., 2021). Variations in precipitation amount and pattern may increase the variability in AET and PET (Goroshi et al., 2017), which will further enhance the evaporative water demand (i.e. ET-Green), reduce the water availability, thereby impacting water security (Gunkel and Lange, 2017). Singh and Kumar (2019) applied the probabilistic Budyko model and quantified changes in the mean annual per capita water availability (PCWA) across India utilizing climate models datasets and projected that the PCWA would decrease in the future with increasing warming. The increasing evaporative water demand and water scarcity conditions will reduce irrigation efficiency and agricultural production in the country. Surendran et al. (2021) elaborated that the increase in temperature is altering the irrigation water requirement in India and this is affecting the agricultural production.

Due to varying climate and landuse/landcover (LULC) conditions, Indian mountain hydrological regimes and in-land river basins are undergoing environmental and socio-economic changes (Poonia et al., 2021; Li et al., 2021). These are inextricably linked to changes in enhanced irrigation water demand and water availability within the river basin (Singh et al., 2021). These changes associated with LULC and climate changes will impact communities, and conversely human management of water resources system (McMillan et al., 2016). The enhanced evaporative water demand (i.e. AET) will increase the over-exploitation of groundwater and diversion of water from one sub-basin to another sub-basin (that is the part of ET-Green) to fulfil the irrigation water requirement and other water demands (e.g. drinking water). These changes in hydrological regimes at a sub-basin scale can pose serious challenges for water availability and demand in India, which may further lead to long-term drought condition (Jha et al., 2019; Sinha et al., 2018). India is among the top growers of agricultural products in the world and the consumption of water for irrigation is amongst the highest (Smilovic et al., 2015). Conventional irrigation techniques cause a huge water loss due to evaporation, percolation, drainage, water conveyance, and extra use of groundwater (Ambika et al., 2016). Therefore, effective LULC and water management practices are needed to mitigate the impact of changing climate on the evaporative water demand and water availability (Singh et al., 2021; Katyaini et al., 2020).

The main objective of this study is to compute the India's evaporative water demand and water availability across 100 river sub-basins (India-WRIS, 2012) by constructing the Budyko framework for sustainable agricultural water management and water availability. In this study, the effect of hydro-climatological changes across 100 river sub-basins have been analyzed during recent past time (2003–2017) by formulating hydro-climatic indices such as EI, DI, and responsivity utilizing the Budyko framework. The changing response of each river sub-basin has been analyzed by characterizing its water demand and availability in terms of ET-Green and ET-Blue. In this study, the Fu's

Budyko equation has been applied to partition the total AET into ET-Green and ET-Blue, which explore the evaporative water demand in different aspects such as the amount of water which is directly available through precipitation, stored water and diversion of water (Fu and Wang, 2019). The Budyko's shape parameter 'ω' has been optimized over 100 river sub-basins and the simulated AET has been computed at each sub-basin to analyze the further changes in India's evaporative demand. The accuracy of the computed AET has been evaluated with the observed AET data points (42 nos.), which shows the applicability of Budyko equations with optimized 'ω' value specific to each sub-basin. To the best of our knowledge, no such study has been performed in India at sub-basin scale which quantifies the India's evaporative water demand and water availability in terms of ET-Green and ET-Blue. For the analysis, the forcing datasets such as AET, PET and precipitation have obtained from the open-source domains such as Global Land Data Assimilation System (GLDAS), Climate Research Unit-Global Data Assimilation System (CRU-GDAS), and Climate Hazards Group InfraRed Precipitation with Station data (CHIRPS), respectively. The applicability of GLDAS AET has been also compared with the available observed AET data.

2. Data utilized

In this study, the GLDAS based AET (Khan et al., 2018; Park and Choi, 2015), and CHIRPS based precipitation datasets have been utilized (2003–2017) at 0.25° × 0.25° grid scale (*ftp://ftp.chg.ucsb. edu/pub/org/chg/products/CHIRPS-2.0/global_daily/netcdf/p25/*). GLDAS can be defined as the terrestrial hydrologic data, including AET and other variables. The GLDAS AET (Version 2.1) is available from the year 2000 to the present time, measured in mm of water loss. GLDAS AET is calculated by NASA using the Noah land surface model (NLSM), run at 0.25° × 0.25° grid scale using satellite and ground-based observational datasets (Khan et al., 2018). Studies which were evaluated the performance of satellite AET datasets showed that the global satellite AET product such as GLDAS has a great potential for global, regional and smaller scale hydrological applications, particularly for the regions having sparse AET observation networks (Pal et al., 2021; Zhan et al., 2019). Previous very few studies have compared the applicability of CHIRPS and other sources of satellite-derived precipitation datasets at India scale (Pal et al., 2021; Gupta et al., 2019) and it was found suitable in capturing precipitation mean and extremes. Hence, in this study the CHIRPS precipitation has been utilized for the analysis. For PET, a CRU based PET high resolution (i.e. 0.25° × 0.25° grid scale.) datasets on the monthly time step for the years 2003–2016 have been utilized. Previously, the applicability of the CRU PET dataset in India was evaluated by Ramarao et al. (2019) and Sonali and Nagesh Kumar (2016) (https://cru data.uea.ac.uk/cru/data/hrg/cru_ts_4.01/cruts.1709081022.v4.01/ pet/).

For the year 2017, the GDAS based PET data (available at 100 × 100 km²) (http://remote-sensing.nci.org.au/u39/public/data/wirada/c mrset/) was utilized after bias correction with reference to the CRU PET dataset. CRU based PET and GDAS based PET datasets have been re-gridded at 0.25° × 0.25° grid scale by followed a methodology used by Singh and Xiaosheng (2019a) and Gupta et al. (2019) to match with the AET and precipitation datasets. For the evaluation of computed AET datasets (as per Fu's equation at sub-basin scale), total 100 sub-basins out of 102 sub-basins have been selected (India WRIS, 2012) (Fig. 1). In this study, two subbasins (No. 49), viz. Drainage Area of Andaman and Nicobar Islands and Drainage Area of Lakshadweep islands (No. 50) have not been considered for the analysis due to unavailability of grid datasets (e.g., Precipitation, AET and PET). The accuracy of computed AET at each sub-basin (total 100 nos.) has been evaluated with reference to observed monthly AET datasets (42 nos.) (measured by lysimeter) distributed across India subbasins (2003–2014) (Fig. 1). The observed AET datasets on the monthly time scale have been obtained from the India Meteorological Department (IMD).
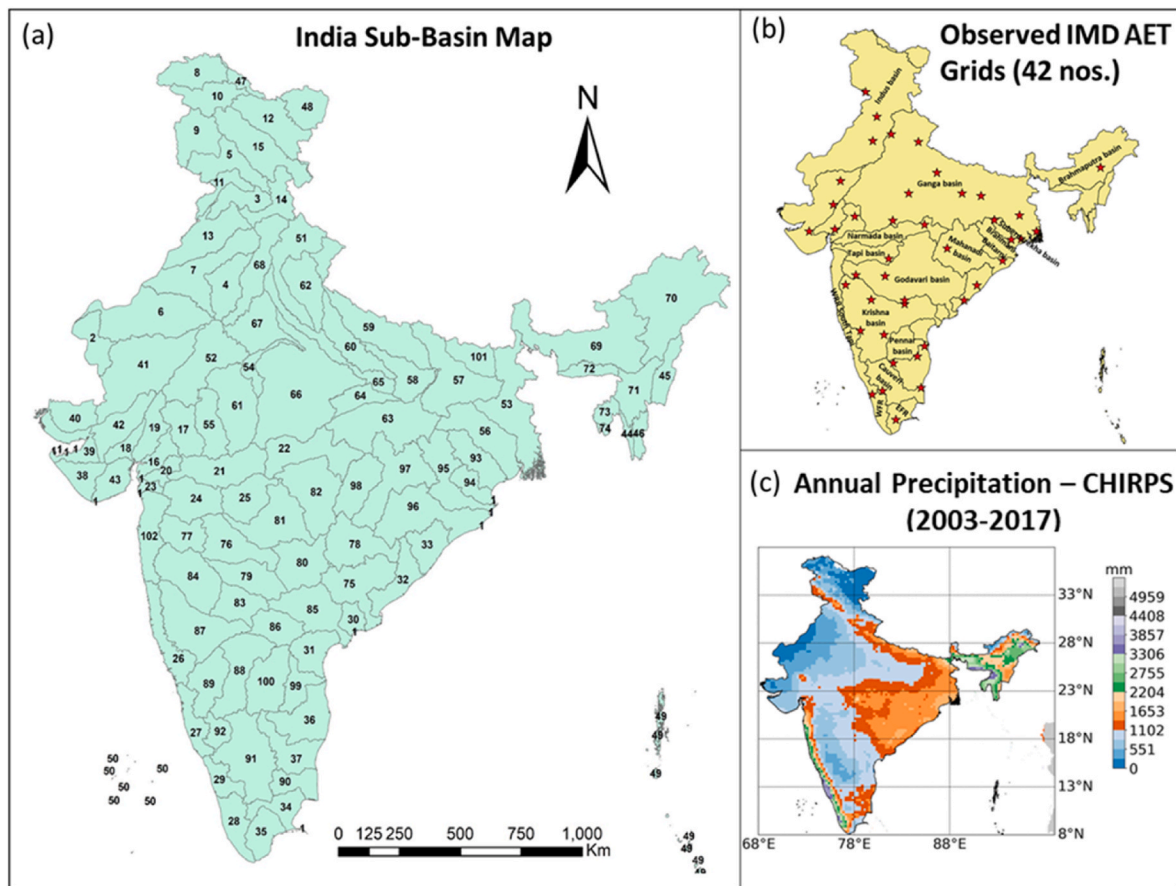
Fig. 1. Study area map highlighting (a) India river sub-basins 102 numbers (as per River Basin Atlas of India by India WRIS), (b) IMD based observed AET data locations along India river basins by India WRIS and (c) annual averaged (2003–2017) Precipitation map as per CHIRPS data..

3. Methodology

3.1. Spatial distribution and seasonal and inter-annual variability in AET and PET

To explore the seasonality in AET across India, the GLDAS AET datasets have been divided into four seasons, viz. June-July-August-September (JJAS), October–November (ON), December-January-February (DJF) and March-April-May (MAM). Then, the AET distribution and patterns as per the above four seasons have been explored across India. The correlation coefficients (R) between annual averaged CHIRPS precipitation (2003–2017) and GLDAS AET (2003–2017) have been computed at each grid scale. Precipitation and temperature variability have been historically considered the main causes for variability of ET in India (Goroshi et al., 2017; Yang et al., 2016). Therefore, a correlation analysis between AET and Precipitation across India was performed to explore AET variabilities associated with precipitation changes. To highlight the inter-annual variability in AET and PET, the AET and PET datasets (2003–2017) were averaged (5-years) and then grouped into three scenarios (i.e. 2003-2007, 2008–2012 and 2013–2017). The percentage (%) of change has been calculated to quantify the magnitude of change in AET and PET (Singh and Xiaosheng, 2019a). Any significant changes in AET and PET (here it is analyzed at grid scale ($0.25° \times 0.25°$)) will affect the evaporative water demand and water availability (can be aggregated at sub-basin scale).

3.2. Budyko framework

In this study, the Budyko framework has been developed to assess India's water availability and evaporative demand at each sub-basin

(100 nos.) in the long term recent past time (2003–2017). Budyko curves have been developed in three intra-annual times, viz., 2003–2007, 2008–2012 and 2013–2017. Scientists have made many efforts to develop the theoretical Budyko equation that describes the relationships between EI vs DI (Fig. 2), and many studies have utilized the Budyko equation and adjusted the equation for different purposes at catchment/basin scale around the world (Fu and Wang, 2019; Gudmundsson et al., 2016). The original Budyko curve equation $F(\Phi)$ can be written as (Budyko et al, 1974) (eq. (1)):

$$F(\Phi) = \left[\frac{PET}{P} tanh\left(\frac{P}{PET} \right) \left(1 - exp\left(-\frac{PET}{P} \right) \right) \right]^{0.5} \quad (1)$$

In Budyko framework, the two most important hydro-climatic indicators, dryness index DI (i.e. PET/P) or aridity index (AI) and evaporation ratio (EI) computed as AET/P, have been computed for each sub-basin. The EI highlights the variations in evaporating demand and DI reflects the dryness condition (Liu et al., 2019). In several studies, the ratio of AET/P was considered a measure of long-term annual average water balance, which separates the AET and Q as per P (Creed et al., 2014). Generally, AET/P should not exceed unity until and unless no additional water is being added into the sub-basin. Here, DI is a ratio of energy available to water availability and defines the long-term mean climate (Fig. 2). In this interpretation, PET/P < 1 can be associated with humid areas where P is significant and energy supply is typically a limiting factor for AET. Contrary to this, PET/P > 1 represents arid regions where P is low and AET could be limited by water supply and this represents water stress or water limited conditions.

In this study, the long-term average deviations in EI and DI from the theoretical Budyko curve have been computed. A relationship has been established between EI and DI, which is termed as 'elasticity (e)' (Creed
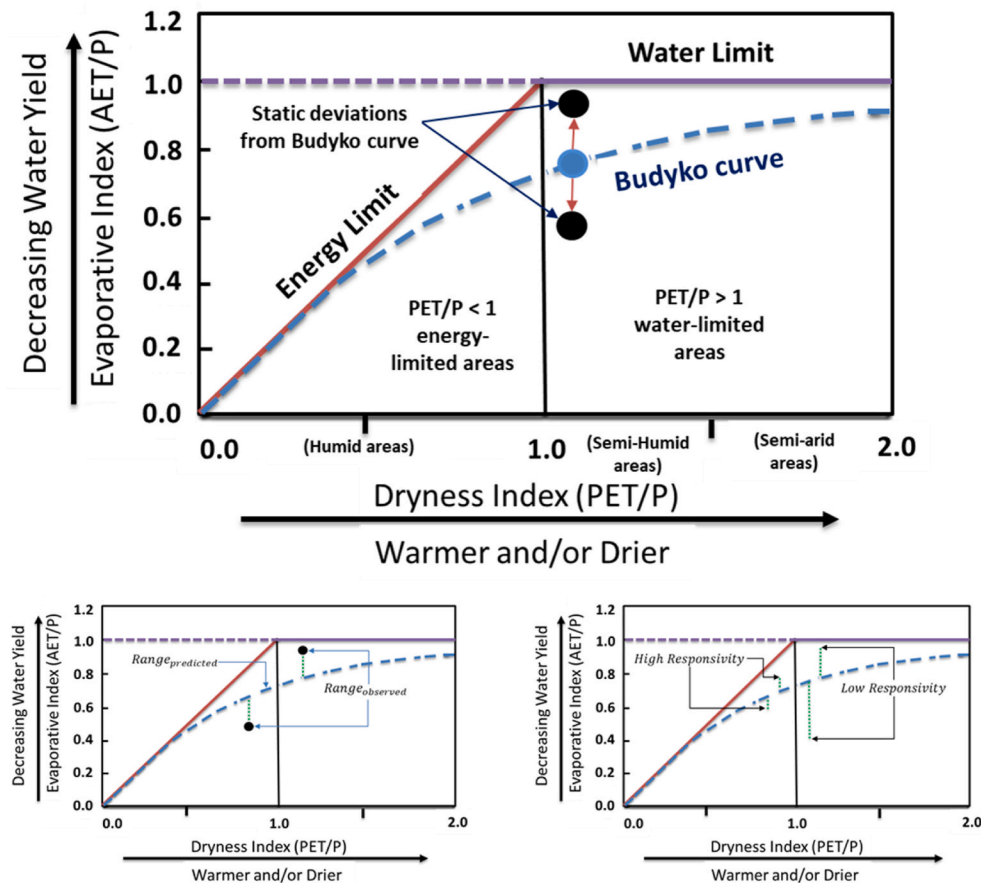
Fig. 2. Explanation of the Budyko curves and their hydro-climatic variables, viz. Evaporative index (EI), dryness index (DI), energy limit, water limit and responsivity.

et al., 2014). Subbasins with higher departures from the theoretical Budyko curve indicate low or no elasticity (Fig. 2). A high elasticity or less deviations represent insignificant hydro-climatological and LULC changes in EI and DI in subbasins and vice-versa (Helman et al., 2017). Whereas, subbasins having low elasticity indicate that they are prone to water scarcity. These river subbasins will have limited ability to adapt to changing climate conditions and can be defined as having low and no hydrological resilience (Helman et al., 2017).

Few studies have performed 'responsivity' analysis under the Budyko framework which been found helpful to determine how the sub-basin can adopt to changing climate and other conditions (e.g. LULC) by linking the connection between water yield (i.e. runoff) from the corresponding sub basin area to the atmospheric conditions (Creed et al., 2014). The responsivity is measured as the maximum range in EI after accounting for natural deviations in the Budyko curve. Responsivity can be categorized as: (a) low responsivity and (b) high responsivity (Fig. 2). Low responsivity implies that water yields in the given area or basins are not synchronized to precipitation (P) and high responsivity describes that water yields are synchronized to P. The responsivity can be calculated as (eq. (2)) (Creed et al., 2014):

$$Responsivity = 1 - \left(Range_{observed} - Range_{predicted} \right) \tag{2}$$

In this study, the responsivity has been mainly measured to analyze the effect of hydro-climatological changes on EI/P across all river subbasins. The responsivity is computed in three intra-decadal years (i.e. by taking the average of five years) compared with the long-term averaged time duration (i.e. 2003-2017).

To quantify the evaporative water demand and water availability, the total AET has been divided into ET-Green and ET-Blue by using the

Budyko framework, which demonstrates an empirical relationship between AET and precipitation for subbasins with the negligible storage changes. As per Simons et al. (2020), ET-Green refers to AET from the precipitation and soil moisture and ET-Blue refers to AET from the water stored in the groundwater or surface sources such as rivers and lakes. In this study, ET-Green and ET-Blue have been computed by the following equations (3) and (4) (Simons et al., 2020):

$$ETGreen = \text{minimum} \quad (F(\Phi) \times P, AET) \tag{3}$$

$$ETBlue = Actual\ ET\ - \ ETGreen \tag{4}$$

In the computation of ET-Green and ET-Blue, some uncertainties can arise because in the Budyko Hypothesis, partitioning of AET into ET-Green and ET-Blue is described by an empirical relation between AET, reference evapotranspiration (ET_0) and precipitation (P) in dynamic equilibrium and with negligible storage changes. The water potential areas (i.e. streamflow or runoff, denoted by Q) have been computed by equation (5):

$$Q = P - AET \tag{5}$$

Here, water potential areas highlight the areas where Q is synchronized to P and such subbasins can adapt hydro-climatological and LULC changes. Subbasins, where P is not sufficiently available, are characterized by water scarce regions. In these subbasins, an additional water is required to fulfill their evaporative water demands.

Different authors have derived multiple equations to further develop a Budyko's framework and improved the efficacy of computational hydro-climatic variables (Fu and Wang, 2019; Gudmundsson et al., 2016; Creed et al., 2014). In Fu's modified Budyko equation (Fu and

Wang, 2019), a dimensionless empirical shape parameter 'ω' has been introduced which can be defined as calibration coefficient to optimize AET for the given sub-basin (equation (6)):

$$\frac{AET}{P} = 1 + \frac{PET}{P} - \left[1 + \left(\frac{PET}{P}\right)^\omega\right]^\omega \qquad (6)$$

where, the shape parameter 'ω' defines the effect of changes in land surface characteristics and climate seasonality on the water-energy balance. In this study, the parameter 'ω' of equation (2) was optimized for 100 river sub-basins with values of Precipitation (P), PET and AET for the long-term time domain (2003–2017). For the optimization of nonlinear Fu's based Budyko equation, the Generalized Reduced Gradient (GRG) method (Smith and Lasdon, 1992) has been applied by utilizing the solver functionality of MS Excel (Lyon et al., 2017). Based on the fitted ω, the AET has been calculated and then compared with the observed AET. The root mean squared error (RMSE) has been calculated across all river sub-basins to validate the applicability of Fu's Budyko equation with optimized ω values. The higher ω values indicate a higher ET-Green under the same PET/P ratio (the aridity index). Therefore, they are related to a greater capacity of a sub-basin to retain water for evapotranspiration.

4. Results and discussions

4.1. Spatial distribution of AET and its correlation with precipitation

Changes in AET can be easily correlated with the changes in the amount of precipitation (Yang et al., 2016). Fig. 3a and b shows the correlation between GLDAS AET and CHIRPS precipitation. The correlation coefficient (R) computed between CHIRPS precipitation and GLDAS AET shows good correlations in most of grids (ranged from −1.0 to 1.0). The negative correlation has been seen mostly in high forest density areas (like Western Ghats) and cold desert region (Jammu & Kashmir and Ladakh) where topography is dominant with snow and glaciers. As per high AET and low AET areas like Rajasthan and North-Eastern region, respectively (Fig. 3a), the correlation coefficient is recorded ≥0.5 and positive (Jhajharia et al., 2009). Fig. 3b shows that for major regions in India, the evaporative demand is mainly dependent on the precipitation. Goroshi et al. (2017) correlated the AET and precipitation datasets across India and observed a strong positive correlation (R > 0.5) over semi-arid and arid regions similar to the above observations (Fig. 3b), whereas, a negative correlation was also observed in a very few dry regions of western India. Overall, our findings suggest that precipitation has significant influence on AET, however in few areas (e.g. humid areas, high forest density areas and cold desert mountainous regions) several other factors may also have enormous influence on the AET. These finding are useful to understand the spatial

distribution of AET and its relationship with precipitation showed in Fig. 3b. These findings may be helpful to explain India's evaporative demand and water scarcity conditions at a very finer scale under the current changing hydro-climatological conditions.

4.2. Spatio-temporal and intra-annual changes in AET and PET

A clear seasonal variation can be observed in AET across India (Fig. 4). India is mostly influenced by South Asia Summer Monsoon (SASM) system and most parts of India receive around 80–85% precipitation during JJAS months (Joseph et al., 2018). However, India has significant diversity in the climatic system from North to South and from East to West. Therefore, precipitation and AET exhibit enormous variability in all seasons across India (Joseph et al., 2018). In Fig. 4, the JJAS based AET ranges from 65 mm to 585 mm, the ON based AET ranges from 0 mm to 252 mm, the DJF based AET varies from 0 mm to 360 mm and MAM based AET ranges from 0 mm to 378 mm. Based on this, one can see that the maximum AET corresponded to monsoon season (i.e. JJAS) in major portions of India, except some desert region (e.g. Rajasthan state) and Jammu & Kashmir (where AET was found less than 195 mm). In winter (DJF) and summer (MAM) seasons, most regions in India have recorded less AET (~160 mm). Considering all seasons, the desert regions of India correspond to lower AET values, while areas in Southern India and North-Eastern India corresponded to higher AET ranges as compared to other areas. Goroshi et al. (2017) studied AET fluctuations and concluded that the seasonal variability in AET is mostly governed by air temperature, wind speed and humidity. Our observations also revealed the same and it can be stated that any significant change in these variables will affect the natural variability of AET across India. A very few studies have shown that the fluctuations in AET values may depend on the variable agricultural cropping patterns and crop varieties (Soni and Singh, 2017). The AET patterns define the terrestrial water budget and exchanges of surface energy that could explain the India's evaporative water demand (mostly through vegetation) in different seasons. Therefore, seasonal and inter-annual variability in AET is crucial to determine the water availability.

As per AET and PET time series data availability (2003–2017), the whole time series data (2003–2017) was divided into three average time series (TS) durations (D) i.e. (TS1): 2003–2007, (TS2): 2008–2012 and (TS3): 2013–2017 (Figs. 5 and 6). Fig. 5a–c shows the spatio-temporal variations in annual AET values across India from the year 2003–2017 in three average TS durations and Fig. 5d–f shows the percentage (%) of change in AET values in three average TS durations i.e. TS1 vs TS2, TS1 vs TS3 and TS2 vs TS3. In Fig. 5, the spatio-temporal changes in AET can be clearly visualized, especially in AET range between (300 mm–1000 mm). The largest change in AET has been recorded between TS2 vs TS3 (Fig. 5f) followed by TS1 vs TS3 (Fig. 5e), which is indicates that very recent past time has seen more critical hydro-climatic changes in India.
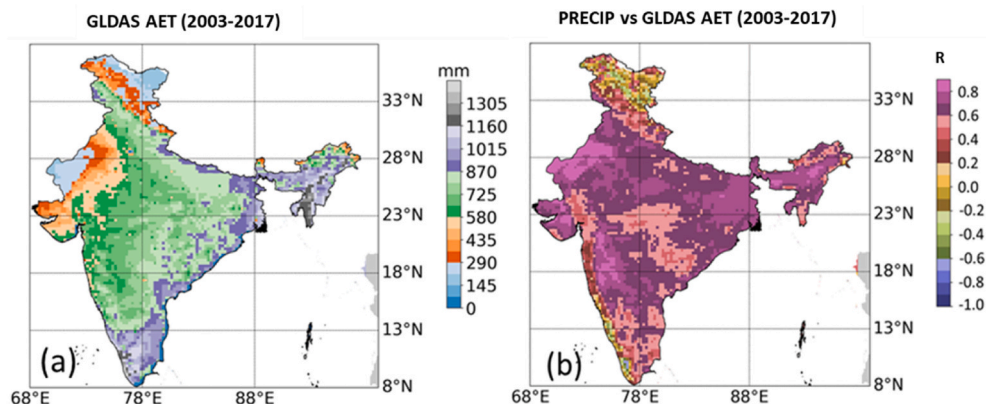

Fig. 3. Highlighting spatial distribution of (a) GLDAS AET (2013–2017) and (b) Correlation between CHIRPS Precipitation and GLDAS AET (2003–2017.
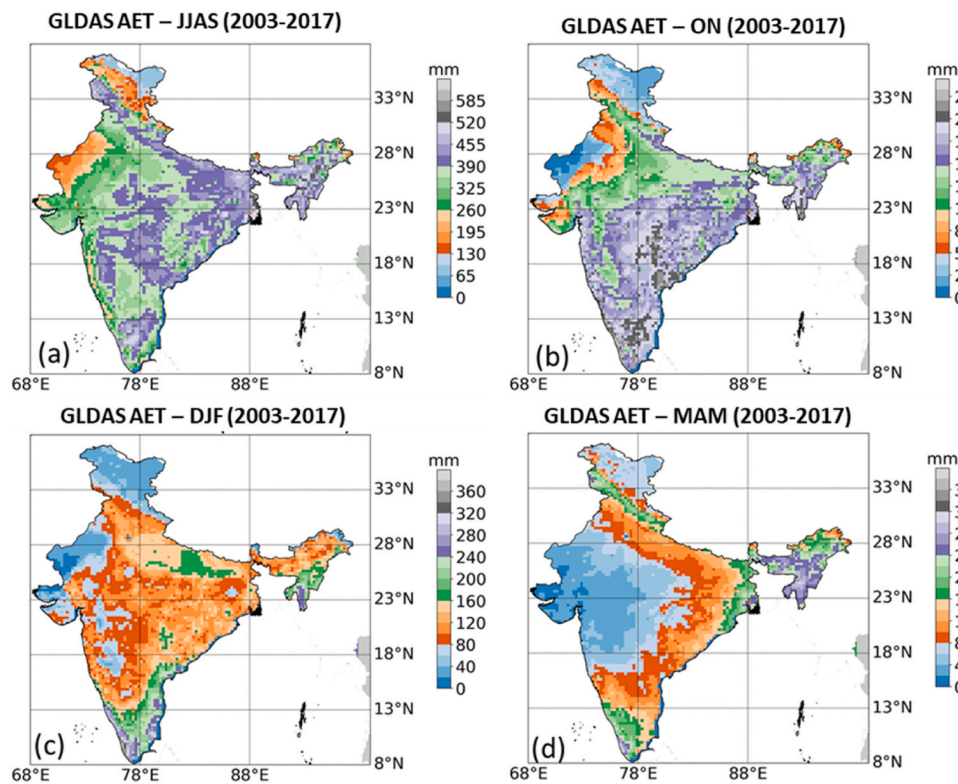
Fig. 4. Seasonal variations in GLDAS AET (2003–2017) datasets: (a) June-July-August-September (JJAS), (b) October–November (ON), (c) December-January-February (DJF) and (d) March-April-May (MAM).

Fig. 5. Intra-annual variations in AET (5-years averaged) highlighting variations across India and change (%) (a) averaged AET (2003–2007) – TS1, (b) averaged AET (2008–2012) – TS2, (c) averaged AET (2013–2017) – TS3, (d) change in AET (2003–2007), (e) change in AET (2008–2012) and (f) change in AET (2013–2017).

In Fig. 5e and f, it can be clearly seen that region such as Western India (mostly desert parts), some parts of Punjab and Haryana, and some areas in Southern India show reduction in AET values but most parts of India shows positive change in AET values (i.e., increase in evaporative demand in those areas). The largest increase in AET was found in Northern India, Western Himalayas, and several areas in Eastern Himalayas, which could be a sign of either increased vegetation or agricultural expansion (as the transpiration is the dominant process controlling AET) or higher increase in temperature (Kundu et al., 2017; Sonali and Nagesh Kumar, 2016). Several studies have analyzed the

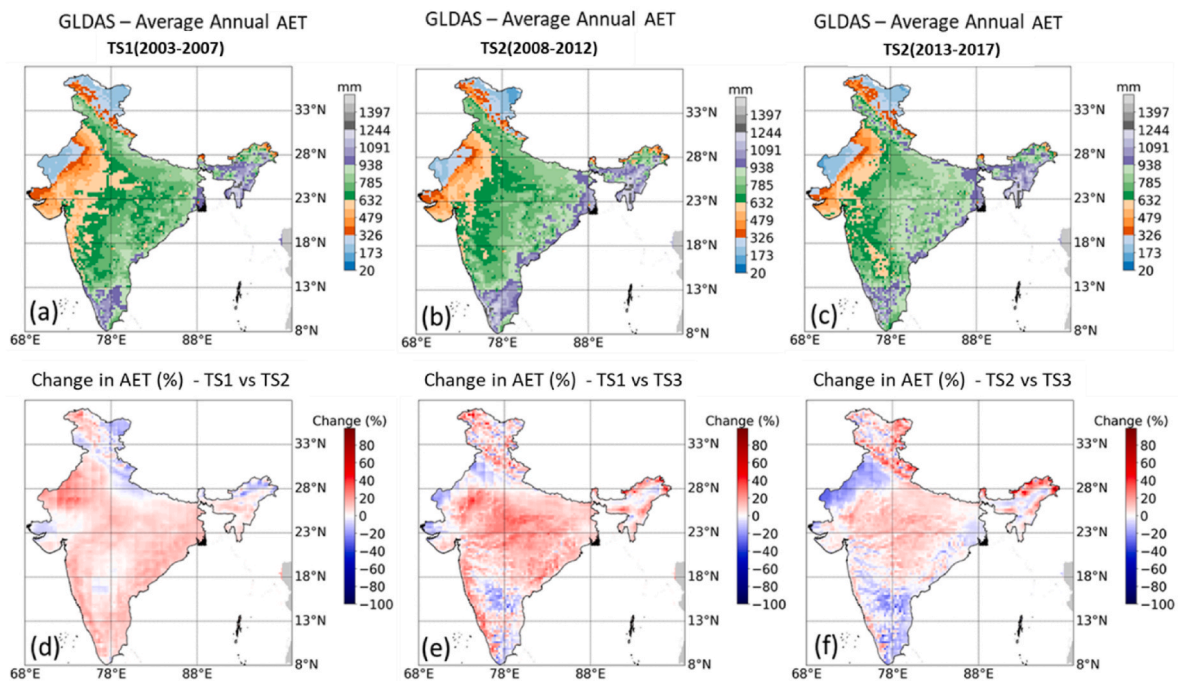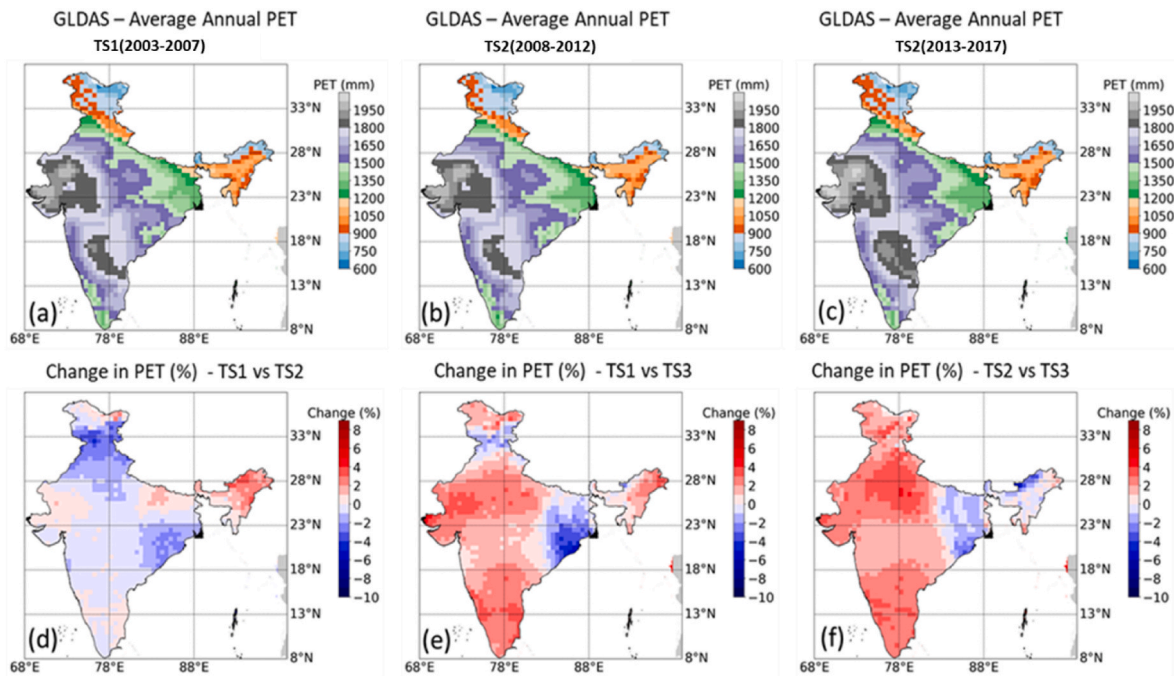**Fig. 6.** Intra-annual variations in PET (5-years averaged) highlighting variations across India and change (%) (a) averaged PET (2003–2007) – TS1, (b) averaged PAET (2008–2012) – TS2, (c) averaged PET (2013–2017) – TS3, (d) change in PET (2003–2007), (e) change in PET (2008–2012) and (f) change in PET (2013–2017).

effect of significant increase of temperature in these areas and the resultant AET rate (Kundu et al., 2018). Fig. 6a–c highlight the spatio-temporal changes in PET across India and Fig. 6d–f demonstrate the percentage of change in PET in 2003–2017 duration scenarios. In India, PET typically ranges from 500 mm to 2000 mm (Singh and Kumar, 2015). As compared to AET, PET shows less rate of change. However, in recent decades (i.e. TS1 vs TS3 and TS2 vs TS3) a noticeable rise is recorded in PET rate in most areas of India except Eastern and North-Eastern parts (decrease in PET) as shown in Fig. 6e and f.

Fig. 7 shows variations in annual AET in the spatio-temporal time durations (2003–2017). For analyzing the annual basis changes in AET, the annual average of the total time series (2003–2017) has been computed and the averaged scenario (i.e. 2003-2017) has been taken as a reference or baseline scenario. Then, with respect to the baseline scenario, the ratio has been computed for each year from 2003 to 2017. As per Fig. 7, as the time year increases, the variability among different scenarios increases. During earlier years (i.e. up to 2009), only small changes were observed in AET (Fig. 7a–g). After 2012, the annual fluctuations in AET values increase and these AET variations can be visualized in Fig. 7h–°. The ratio-based plots after 2012 (Fig. 7k–°), showed large variations in AET across India; illustrating that in the last few years the rate of change of AET is significantly enhanced. Overall, a ratio-based plots showed considerable variations in AET across India during 2003–2014 and very recent past years (2015–2017) have shown extensive changes in AET across India. Similar observations have also elaborated in previous studies done at India level assessment of AET (Kundu et al, 2018; Soni and Singh, 2017). Soni and Singh (2017) demonstrated about the causes of AET fluctuations and computed positive trends in reference crop ET indicate that the water demand required for different crops in various seasons will increase. Kundu et al. (2018) found a significant variation in seasonal AET, and as expected, high AET is observed over water bodies and forest areas, especially during the pre-monsoon season (MAM).

4.3. Budyko analysis for long-term water partitioning into ET

To estimate the India's evaporative water demand and water availability (i.e. the portioning of precipitation into AET & Q) for 100 river

sub-basins, the Budyko curves have been developed for individual sub-basins. In Budyko curves, each river sub-basin describes the characteristics of landscape regarding energy and water balance. In Budyko framework, DI and EI have been computed to assess the water availability and scarcity across all sub-basins. In Fig. 8a–d, the observation data points (each point represents a river sub-basin) are shown in Green colour. In these figures, for the river sub-basins with PET/P < 1, the energy supply is the limiting factor for AET. As compared to averaged Budyko curves (Fig. 8b–d), the distribution of AET/P (i.e. EI) shows an enormous variation during 2003–2007 (Fig. 8b) and proportioning for the higher AET in Budyko curves than that of 2008–2012 (Figs. 8c) and 2013–2017 (Fig. 8d). As per the plotted Budyko curves in different TS durations, the EI and DI showed significant deviations from the theoretical Budyko curve line. Each time slice exhibited a different pattern of changes in DI and AI and showed a distinctive variation during 2003–2017. In India, each river sub-basin represents a unique topography and climate (India-WRIS, 2012). Many past studies have shown the effect of climate change in the hydro-climatology of Indian river basins (Singh et al., 2010; Singh and Kumar, 2015) (Fig. 8a to d).

In Budyko curves (Fig. 8a–d), the DI differentiates the sub-basins into humid and dry conditions. Basins corresponded to PET/P > 1 represent dry conditions; while the sub-basins with PET/P < 1 represent the humid (or wet conditions). Under humid conditions, AET will scale almost linearly with PET (i.e., evaporative demand), but in arid conditions where the supply of moisture is limiting, AET is constrained by P and is mostly independent of PET (Simons et al., 2020). Most of the observation points show DI > 1 (warmer or drier conditions), illustrating water stress conditions in many sub-basins. In Figs. (8a to 8c), as time progress (from 2003 to 2017), a consistent increase in the DI has been recorded (Fig. 8d). Creed et al. (2014) explained that the increase in DI (or horizontal changes in Budyko curve) reflects a change in the climatic conditions due to changes in precipitation and temperature. Based on the resultant observations from the Budyko curves, it can be concluded that the changes in EI and DI are noticeable and can be linked to LULC and climate changes. DI and EI changes will affect the future water availability in sub-basins.

Fig. 9 (a, e, i, m) represent the relationship between P versus EI during 2003–2017 (Figs. 9a), 2003–2007 (9e), 2008–2012 (9i) and
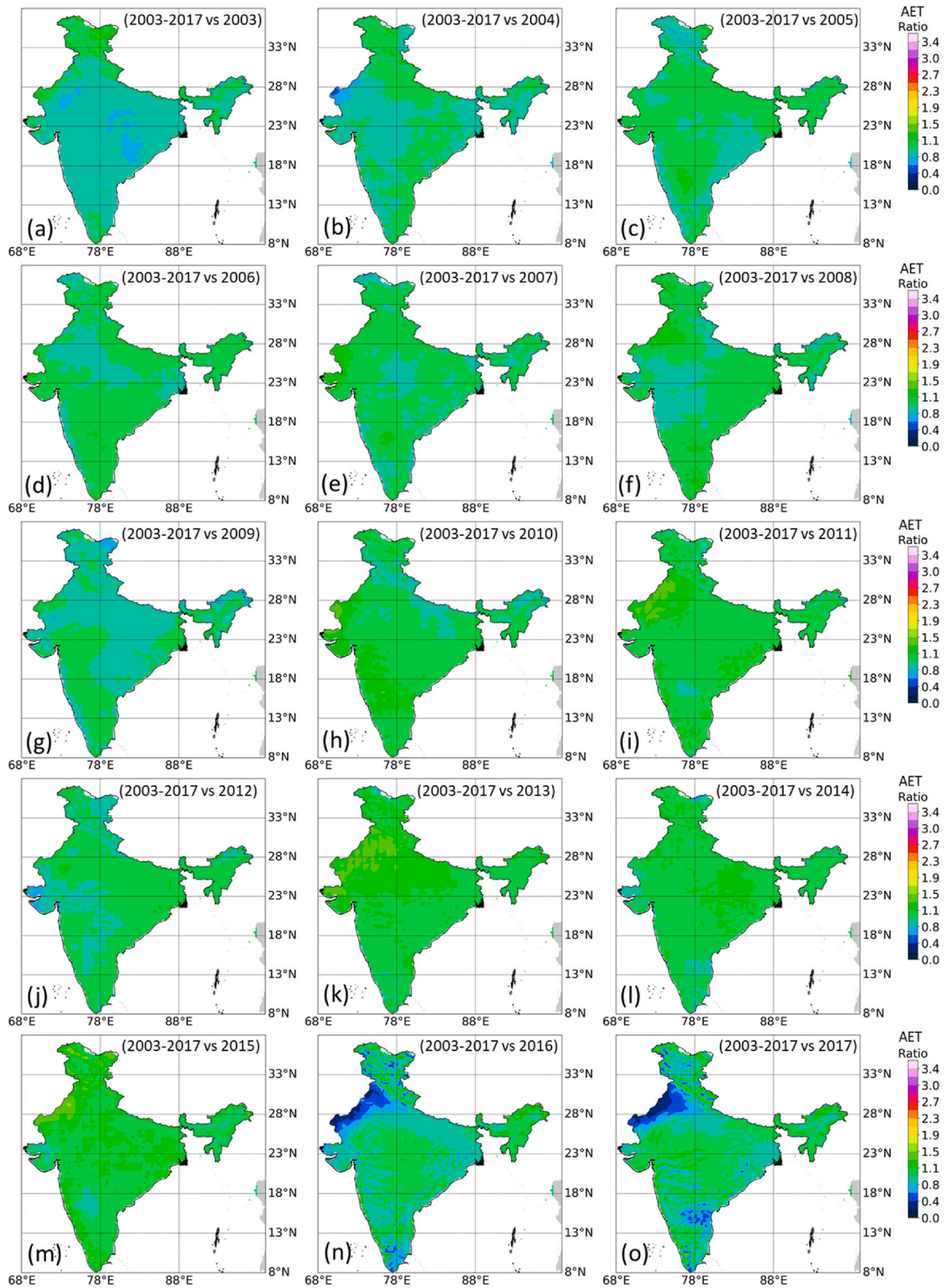
Fig. 7. Highlighting Annual fluctuations (a to f) in AET (2003–2017) computed with reference to (a) average AET (average of 2003–2017) using GLDAS AET datasets.
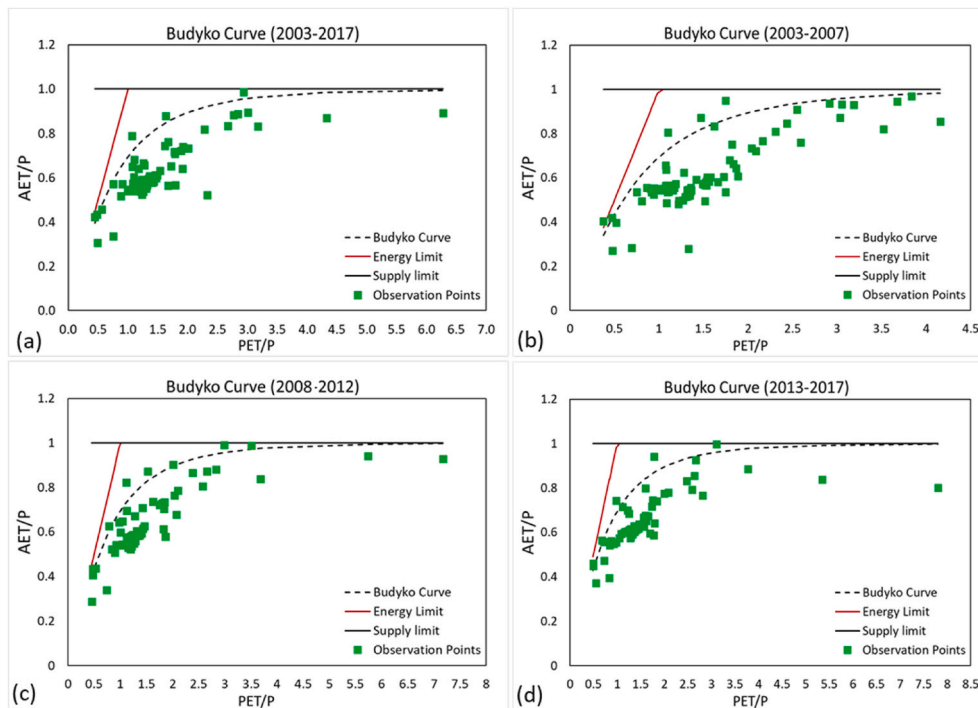
Fig. 8. Budyko index showing variations in India's evaporative water demand in form of EI and DI in three 5-years averaged durations: (a) D1-2003-2007, (b) D2-2008-2012, (c) 2013–2017 and one long-term durations (d) 2003–2017 to highlight the recent changes.
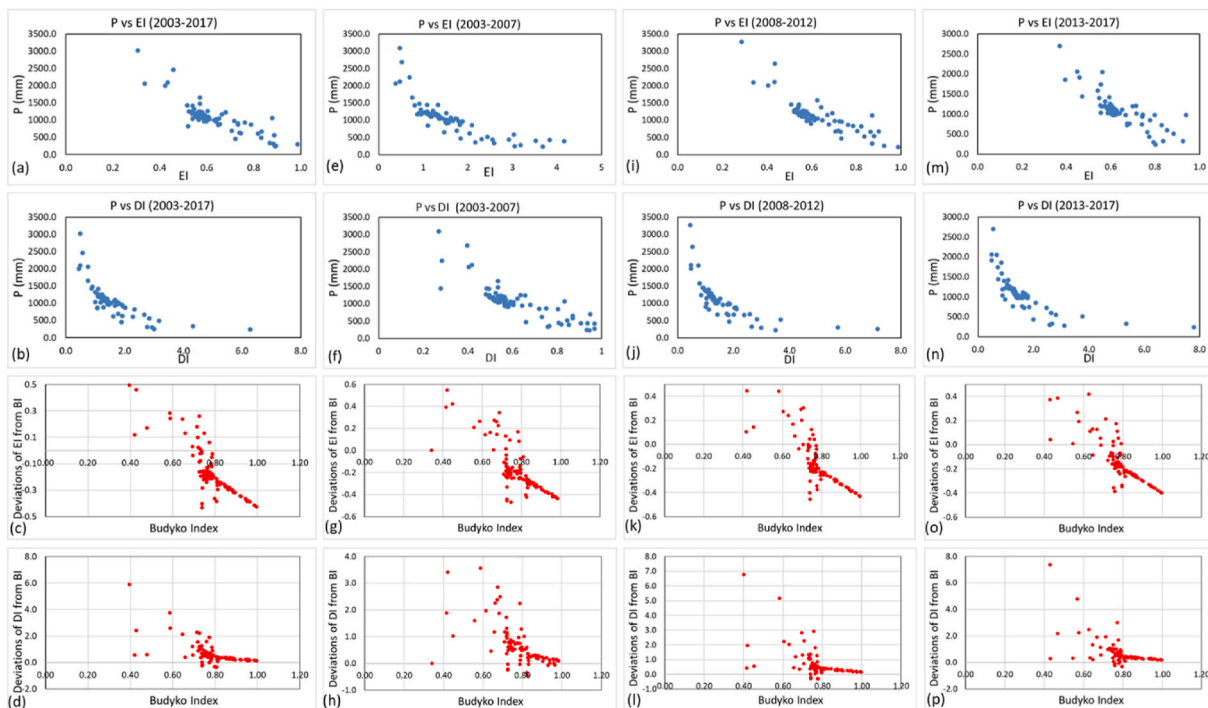
Fig. 9. Relationship between precipitation (P) vs. EI (a, e, i, m) and DI (b, f, j, n) in 5-years averaged durations compared to long-term scenario (2003–2017), (c, g, k, o) deviations of EI from Budyko curves and (d, h, l, p) deviations of DI from Budyko curves compared to long-term scenario (2003–2017).

2013–2017 (9m), respectively. Similarly, Fig. 9 (b, f, j, n) represent the relationship between P versus DI during 2003–2017 (Figs. 9b), 2003–2007 (9f), 2008–2012 (9j) and 2013–2017 (9n), respectively. Figs. (9a, 9e, 9i, 9m, 9b, 9f, 9j and 9n) clearly highlight that several observation points (i.e. sub-basins) show an enormous fluctuation, which have occurred due to variations in the total precipitation that has

fallen and this fact can be revealed while seeing the variations in EI and DI values (Fig. 9). Based on the average annual precipitation pattern, Indian regions are categorized into arid to wet regions such as desert areas corresponded to low rainfalls (~200 mm–500 mm) and North-Eastern states like Meghalaya corresponded to wet regions (>5000 mm) (Fig. 1). Compared to Fig. 9a, the diagrams for P vs EI (Fig. 9e, 9i

and 9m) look more scattered, because AET has shown a significant spatial variation across India (Figs. 3 and 4). In Fig. 9f, the DI ranges up to 1, while Fig. 9j and n shows that there is an increase in DI over low to moderate precipitation areas (<1000 mm). These observations support the above findings (Fig. 8) and we may conclude that in many sub-basins, precipitation deficit has increased in recent past.

Figs. (9c, 9g, 9k and 9o) illustrate deviations of EI from the theoretical Budyko curves plotted in three averaged (5 years) durations (2003–2017, 2003–2007, 2008–2012, 2013–2017) respectively. Similarly, Figs. (9h, 9l, 9p and 9d) demonstrate the long-term average deviations of DI from the Budyko curves in three averaged times series. In Figs. (9g, 9k and 9o), a clear shifting in EI range from the theoretical Budyko curve can be observed during 2003–2007, 2008–2012, 2013–2017, as compared to the long-term scenario (2003–2017) (Fig. 9c). This shifting elaborates about the changes in AET with respect to P and this can be attributed to hydro-climatological changes in sub-basins. However, as per Fig. 2, ideally, the observation points should follow the theoretical Budyko curve line, which represent the no-change condition. Creed et al. (2014) explained that sometimes due to the inadequate representation of AET and climate change, which may have significant effect on the hydro-meteorological characteristics of sub-basins for those sub-basins observation points fall off the theoretical Budyko curve. In Fig. 9c, 9g, 9k and 9o, the negative shift shows a downward shift and decrease in AET and increase in runoff (Q), while positive shift represents an upward shift and increase in AET and decrease in Q. These deviations highlight the effect of LULC and hydro-climatological changes in sub-basins and their effects on EI (with respect to AET and P). These changes in sub-basins may disturb the synergy between India's evaporative water demand and water availability. Similar conclusions were made in few studies in India, which demonstrated the effect of climate change in India's water availability (Katyaini et al., 2020). Based on the above observations (Fig. 9c, 9g, 9k and 9o), it is concluded that majority of river sub-basins in India show an increase in AET rate, which might be caused by due to increasing warming across India (Singh and Kumar, 2019). As per Fig. 6, changes in AET from 2003 to 2017 support the above observation.

In Figs. (9d, 9h, 9l and 9p), the static deviations (or vertical displacements) of DI from the Budyko curve show the inherent characteristic of each river sub-basin in India. Vertical deviations from the Budyko curve ranged from −2 to 8, -1 to 4, -1 to 8 and -2 to 8 for the long-term duration (i.e. 2003-2017) and three averaged time periods (2003–2007, 2008–2012 and 2013–2017), respectively. According to Creed et al. (2014), grids with deviation<0 exhibited a pre-warming water yield, which are found to be higher than expected yield revealed by the Budyko's theoretical predictions. Although, grids with deviations>0 exhibited a lower water yield than expected, while grids falling near the curve (|deviations|<0.05) indicated a pre-warming water yield that were consistent with the theoretical predictions of the Budyko curve. The variation in static deviations (the shifting of DI ranges from the Budyko curve) can be seen in all durations (Fig. 9d, 9h, 9l and 9p). Considering the deviation of DI from the Budyko curve (i.e. −2 to 8) in case of Figs. 9l and p as compared to Fig. 9h, this confirms that the dryness is continuously increasing in many river sub-basins of India. The rate of change of DI versus sub-basins revealed the same as shown in Table 1. Based on these observations, it is understood that sub-basins may be critical in fulfilling the evaporative water demands and facing water scarcity conditions due to reduction in the amount of precipitation

Table 1
Rate of change of DI values versus sub-basins in different time slices viz., 2003–2007, 2008–2012, 2013–2017.

Time	No of Subbasins with DI > 1	Maximum DI
2003–2007	83	4.1
2008–2012	85	7.1
2013–2018	86	7.8

(Gupta et al., 2019) and high evaporative water demand.

Fig. 10 shows the responsivity based observations which have calculated in the three averaged (5-years) and long-term TS series scenarios (i.e. 2003-2007, 2008–20012, 2013–2017 and 2003–2017) at each river sub-basin. In this study, responsivity has been calculated to highlight the deviation of AET/P from the Budyko curve after accounting for natural deviation in the Budyko curve (Fig. 2). The long term averaged responsivity scenario (2003–2017) can be considered as the reference scenario to compare the other TS scenarios to account changes in AET/P. In Fig. 10, large deviations with low responsivity can be seen in all three scenarios. As per the comparisons, the deviations have been increased during the times 2008–2012 and 2013–2017, when compared to 2003–2007 based scenario and long-term series (2003–2017). These changes or shifts in the EI values (for each river basin) could be useful in the identification of sensitive river sub-basins that are undergoing fundamental changes in response to global change (Creed et al., 2014).

In Fig. 10, river sub-basins with low responsivity (i.e. ~0.5–0.8) stay on the theoretical Budyko curve, while river sub-basins with high responsivity (i.e. >0.8) underwent substantial changes in the partitioning of water from higher ET (low water yield) to lower ET (high water yield) or vice versa, which elaborate the hydro-climatological changes in response to shifts in climatic conditions (Creed et al., 2014). In Fig. 10, one can clearly see that most of the river sub-basins, parts of Northern India and Southern India corresponded to high responsivity. Similar, observations are also observed for river sub-basins parts of western part of India, mainly a major part of the Gujarat and Maharashtra. As per the findings from Figs. 8–11, it is concluded that many river sub-basins are becoming drier and reducing water yields (i.e. Q) due to enhanced evaporative water demand under warming conditions. These findings also illustrate that these sub-basins have experienced significant changes in the partitioning of water from higher AET to lower AET or vice versa in reaction to alterations in climatic conditions.

4.4. Assessment of ET-Green and ET-Blue

To determine the India's actual evaporative water demand (i.e. water usability) at the sub-basin scale, the AET was partitioned into ET-Blue and ET-Green during 2003–2017 (in recent past) (Fig. 11a) for each river sub-basin. ET-Green and ET-Blue assume that apart from precipitation, several alternative sources are available to meet the water demand. Fig. 11a shows that many river sub-basins corresponded to ET-Blue (e.g. 1–9, 11–15, 17, 27, 35, 49–50, 66–67) and it means that these river sub-basins are receiving water from external sources like canal water supply or diversion from another basin to fulfil their evaporative water demand (Pingale et al., 2016). The amount of ET-Blue varies from one river sub-basin to another (Fig. 11a). Sub-basins such as 2–4, 15, 27, 35 corresponded to high ET-Blue values than other sub-basins. The details of these sub-basins are given in Table 2.

In cold desert region (river sub-basins such as 8–12, 15 and 47) (e.g. sub-basins belong to Laddakh and Jammu & Kashmir), due to presence of permafrost, the soil moisture is getting enhanced. Therefore, AET can be higher than P in such sub-basins, and the corresponding AET demand will be from ET-Blue. Even though, the desert regions of India such as Rajasthan/Chambal sub-basins receive comparatively low annual precipitation (200 mm–500 mm), but due to high temperature and additional moisture from groundwater, the AET turns out to be greater than the precipitation (Byrne and O'Gorman, 2015; Paulo et al., 2012). In such cases, AET process transformed from water-limited to energy-limited and resulted a significant increase in AET, especially in arid and semi-arid areas (Fig. 2) where energy is not a limiting factor (Cao et al., 2014). In some areas like in Chambal, where agriculture is also dependent on groundwater storages in the absence of significant amount of precipitation, the additional evaporative water demand (or AET demand) is fulfilled by irrigation from groundwater storages and
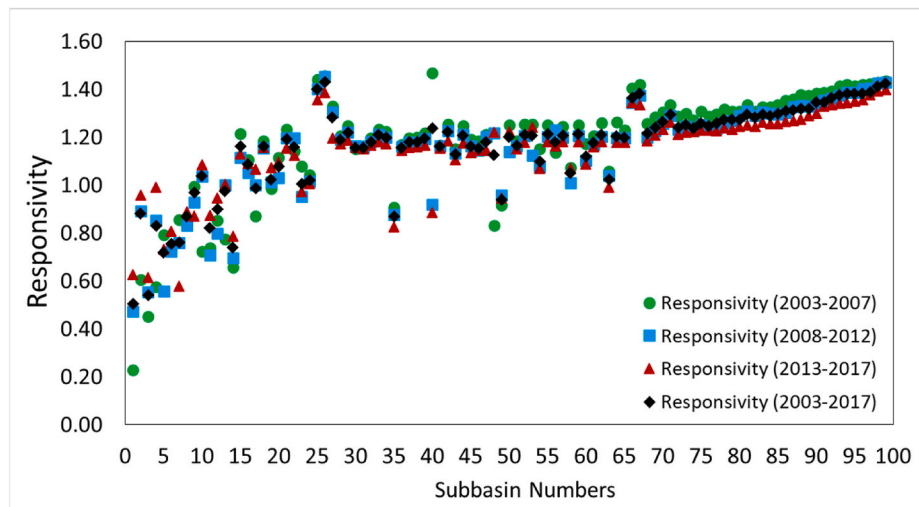
Fig. 10. Responsivity (at y-axis) in different temporal durations highlighting variations across all the sub-basins (at x-axis).

similar observations are recorded in this study (e.g. river sub-basins such as 4 and 52 are corresponded to ET-Blue) (Singh et al., 2010; Schmidt et al., 2009). Apart from this, several river sub-basins (e.g. 69 and 70) receive high precipitation and report high ET-Blue, but that does not mean that these sub-basins are water deficit. The presence of ET-Blue in these sub-basins may be due to high runoff rates and low infiltration along with specific cropping patterns that largely depend on the springs and diverted water from the river (Lahiri, 2019).

Fig. 11b shows the sub-basin wise spatial distribution of ET-Green, ET-Blue (demand side) and water yield (water availability). The ranges of ET-Green in sub-basins vary from ~50 mm to 1000 mm, whereas ET-Blue varied from ~5 mm to 260 mm. In Fig. 11a and b, the maximum ET-Green (in mm) corresponded mostly to moderate to high rainfall areas like North-Eastern States part of Brahmaputra basin (e.g. river sub-basins such as 69–70) and western Ghats (e.g. river sub-basins 27–29), whereas Jammu and Kashmir, Himachal Pradesh, several areas of the desert region (e.g. Rajasthan, Gujarat) and few areas of Southern India recorded low ET-Green (e.g. river sub-basins 2–17). So as per the presence of ET-Green, it can be concluded that in case of moderate to high precipitation induced river-sub basins across India (say precipitation >500 mm), most of the precipitation amount is utilized in agricultural production or intercepted by crops and trees. A significant variation in ET-Green will directly affect the rain-fed crop production and the corresponding area's water availability (Simons et al., 2020). This study shows that around ~50–60% of the water from precipitation turns into ET-Green in India.

The water potential (where sufficient water yield is available) and stress in river sub-basins (where water yield is low) can be visualized in Fig. 11b based on the spatial distribution of ET-Green, ET-Blue and water yield. In Fig. 11b, one can see that the river sub-basins such as 2, 4, 7–15, 24, 25, 52 and 66 are correspond to insufficient water yield. It is concluded that ET-Blue sub-basins have more water demand than ET-Green sub-basins, where P is not sufficient to fulfil the demand and it depends an additional source as discussed above. Therefore, ET-Blue component could be more sensitive to precipitation changes as compared to the ET-Green component. The river sub-basins corresponding to high ET-Blue may have insufficient water to fulfill the demand required for crop production and other vegetation. The above observations clarified that these sub-basins are fulfilling their agricultural demands by utilizing Blue waters (additional sources of water like river, water stored in lakes, ponds and diversion from canal), that is increasing ET-Blue component (Simons et al., 2020). These findings suggest that the increase in ET-Blue within the sub-basins and may affect the overall water availability and enhance the water scarcity in case of

increasing DI.

4.5. Parameterization of Fu's budyko model for different sub-basins in India

Fu's 'ω' describes the characteristics of each river sub-basin based on the land cover, soil hydraulic properties, vegetation and climate. As discussed in Section 3.2, the Fu's Budyko model was parameterized and the optimized values of Fu's 'ω' for all 100 river basins across India are given in Table 2. No such ω values have been developed previously, especially at a small sub-basin scale in India. The ω is computed for the three different averaged years (ω1 for 2003–2007, ω2 for 2008–2012 and ω3 for 2013–2017) and based on the average of ω1, ω2 and ω3, ω4 has been optimized for the whole time series (i.e. 2003-2017). The ω4 values vary from 0.54 to 2.15, which shows a large spatial variability. The higher ω values mostly correspond with high ET-Green. The range of ω computed in this study is comparable to the previous studies (Bai et al., 2020; Singh and Kumar, 2015). Using the optimized ω4 values for all 100 river sub-basins, AET is simulated for all 100 river sub-basins by utilizing the Fu's equation. Then the simulated AET is compared with the observed AET during 2003–2017. For the evaluation, the root mean squared error (RMSE) between simulated and observed AET has been computed as shown in Fig. 12. The satisfactory range of RMSE can be case specific; lower RMSE indicates high accuracy and higher RMSE represents low accuracy (Gupta et al., 2019; Shrestha et al., 2017). In this study, the simulated AET was found comparable with the observed AET and the RMSE varied from 0.00 to 325. For majority of river basins (>75 numbers), RMSE was less than 50 Utilizing Fu's equation and the optimized ω values, future water demand in terms of ET-Green and ET-Blue fractions can be computed if either P or ET is known.

5. Conclusions

This pan-India study was concerned with the assessment of changes in evaporative demand and water availability in recent times by partitioning the actual ET into ET-Green and ET-Blue by using the Budyko theory and open source satellite datasets. The study shows that the largest increase in AET is found in Northern India, Western Himalayas, and several areas in Eastern Himalayas, which could be a sign of either increased vegetation or agricultural expansion (as the transpiration is the dominant process controlling AET) or higher increase in temperature. Ratio-based plots analysis shows considerable variations in AET across India during 2003–2014 and very recent past years (2015–2017) have shown extensive changes in AET across India. The Fu's Budyko

(a)

(b)
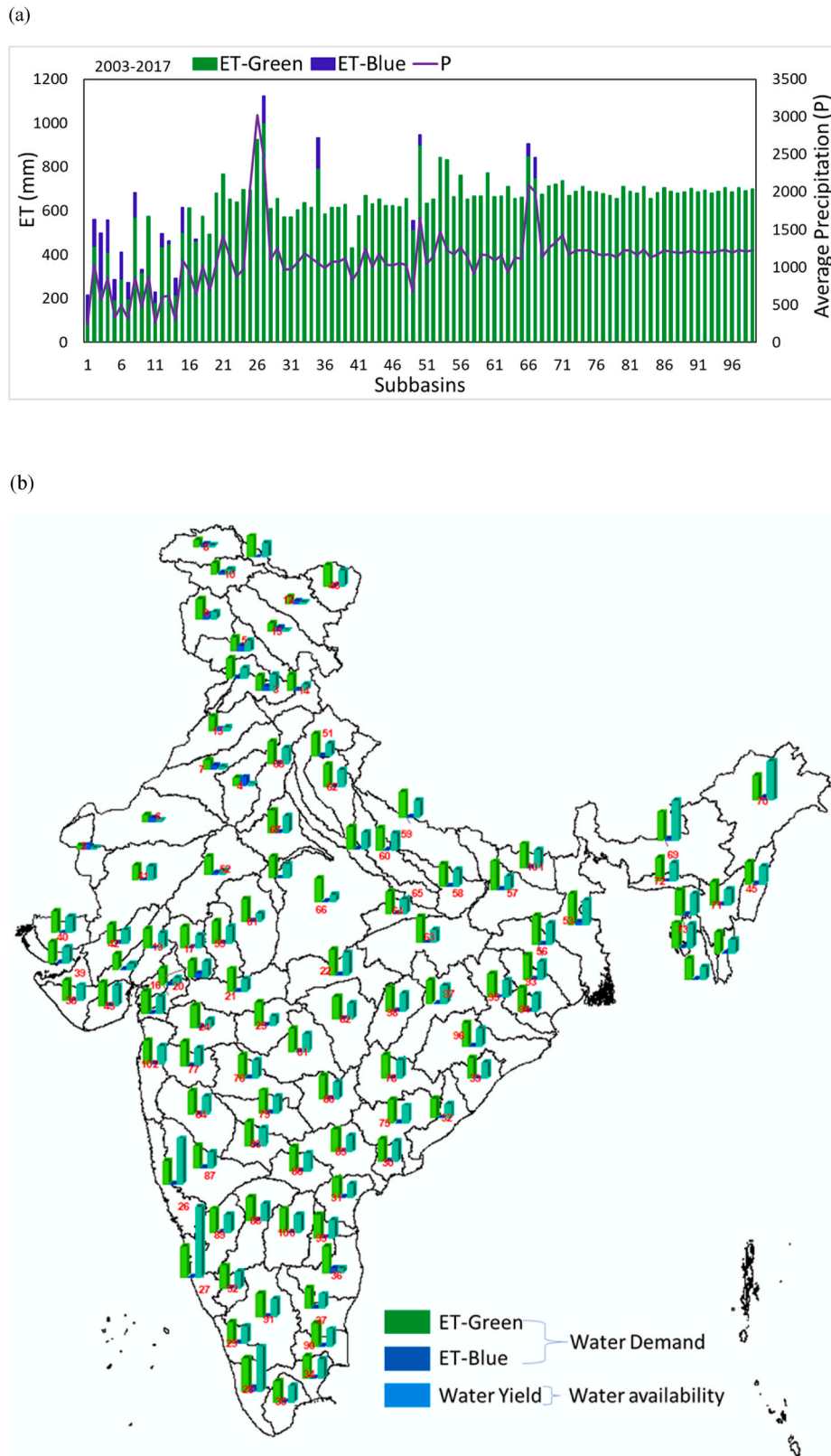
Fig. 11. (a) Budyko based computation of Precipitation (P), ET-Green and ET-Blue highlighting changes across all sub-basins computed during long-term averaged years i.e. 2003-2017 and (b) water demand and water availability at each river basin in terms of ET-Green and ET-Blue.

model has been parameterized for all the 100 river sub-basins of India by optimizing the shape parameter (ω) (vary from 0.54 to 2.15), reflects an enormous variability across all the sub-basins. The number of the sub-basins having DI > 1 are found to increase in the recent time times

along with an increase in the DI values up to 7.8. This shows that the dryness is continuously increasing in many river sub-basins of India. The responsivity analysis shows that the responsivity is decreasing from the 2003 to 2017 and in most of the cases, the responsivity is lower for the

Table 2

Showing the optimized Fu's Budyko shape parameter 'ω' across each river sub basin in the long-term (2003–2017) and three averaged durations series (i.e. 2003-2007, 2008–2012, 2013–2017).

Subbasin	Name of River (sub basin)	Latitude	Longitude	2003–2017	2008–2012	2013–2017	Fitted (2003–2017)
				ω 1	ω 2	ω 3	ω 4
sub-2	Barmer Sub Basin	26.538	70.451	0.42	0.78	0.42	0.54
sub-3	Beas Sub Basin	31.872	76.422	1.53	1.36	1.32	1.40
sub-4	Chautang and others Sub Basin	28.812	75.977	0.95	1.47	1.31	1.25
sub-5	Chenab Sub Basin	33.107	75.770	1.73	1.43	1.39	1.51
sub-6	Churu Sub Basin	27.556	72.759	1.65	0.75	0.76	1.05
sub-7	Ghaghar and others Sub Basin	29.304	74.928	0.90	1.23	1.24	1.12
sub-8	Gilgit Sub Basin	36.364	74.220	1.34	1.31	1.13	1.26
sub-9	Jhelum Sub Basin	34.105	74.432	1.68	1.71	1.59	1.66
sub-10	Lower Indus Sub Basin	35.543	74.942	2.11	2.09	1.85	2.02
sub-11	Ravi Sub Basin	32.259	75.649	1.19	1.48	1.64	1.44
sub-12	Shyok Sub Basin	34.673	77.829	1.14	1.02	1.34	1.17
sub-13	Sutlaj Lower Sub Basin	30.545	75.058	1.02	1.83	2.09	1.64
sub-14	Sutlaj Upper Sub Basin	31.913	77.939	1.37	1.61	1.54	1.51
sub-15	Upper Indus Sub Basin	33.794	77.182	1.10	1.17	1.30	1.19
sub-16	Mahi Lower Sub Basin	22.545	73.372	1.37	1.75	1.56	1.56
sub-17	Mahi Upper Sub Basin	23.567	74.341	2.13	1.75	1.77	1.88
sub-18	Sabarmati Lower Sub Basin	22.817	72.007	1.43	2.15	1.69	1.76
sub-19	Sabarmati Upper Sub Basin	23.480	73.042	1.49	1.69	1.60	1.60
sub-20	Narmada Lower Sub Basin	21.992	73.642	1.80	2.03	1.64	1.82
sub-21	Narmada Middle Sub Basin	22.183	76.017	1.60	2.10	1.61	1.77
sub-22	Narmada Upper Sub Basin	22.769	79.535	1.32	1.37	1.42	1.37
sub-23	Tapi Lower Sub Basin	21.385	73.082	1.52	1.37	1.55	1.48
sub-24	Tapi Middle Sub Basin	20.998	74.799	2.05	1.72	1.74	1.84
sub-25	Tapi Upper Sub Basin	21.114	77.003	1.97	2.19	2.28	2.14
sub-26	Vasishti and others Sub Basin	15.916	74.058	1.17	1.21	1.25	1.21
sub-27	Netravati and others Sub Basin	13.006	75.175	1.18	1.19	1.25	1.21
sub-28	Periyar and others Sub Basin	9.450	76.844	1.28	1.31	1.41	1.33
sub-29	Varrar and others Sub Basin	10.970	76.328	1.37	1.39	1.44	1.40
sub-30	East flowing rivers between krishna and Godavari Sub Basin	16.781	81.195	1.32	1.36	1.42	1.37
sub-31	East flowing rivers between krishna and Pennar Sub Basin	15.635	79.692	1.47	1.44	1.47	1.46
sub-32	Nagvati and other Sub Basin	18.146	82.979	1.45	1.44	1.48	1.46
sub-33	Vamsadhara and other Sub Basin	19.378	84.255	1.39	1.40	1.45	1.41
sub-34	Pamba and others Sub Basin	10.035	78.456	1.34	1.37	1.43	1.38
sub-35	Vaippar and others Sub Basin	9.137	77.849	1.36	1.39	1.44	1.40
sub-36	Palar and other Sub Basin	13.228	79.376	2.10	2.03	2.22	2.11
sub-37	Ponnaiyar and other Sub Basin	12.121	78.792	1.45	1.45	1.49	1.46
sub-38	Bhadar and other west flowing rivers Sub Basin	21.637	70.329	1.40	1.42	1.46	1.42
sub-39	Drainage of Ran Sub Basin	22.851	69.753	1.40	1.42	1.46	1.42
sub-40	Luni Lower Sub Basin	23.792	69.790	1.37	1.40	1.46	1.41
sub-41	Luni Upper Sub Basin	25.649	72.526	1.17	0.98	0.96	1.04
sub-42	Saraswati Sub Basin	23.568	71.761	1.49	1.46	1.50	1.48
sub-43	Shetranjuli and other east flowing rivers Sub Basin	21.561	71.580	1.34	1.36	1.43	1.38
sub-44	Karnaphuli and Others Sub Basin	22.933	92.548	1.51	1.51	1.61	1.55
sub-45	Imphal and others Sub Basin	25.040	94.326	1.36	1.39	1.45	1.40
sub-46	Mangpui Lui and others Sub Basin	22.918	93.023	1.45	1.46	1.53	1.48
sub-47	Shaksgam Sub Basin	36.103	76.326	1.49	1.49	1.53	1.50
sub-48	Sulmar Sub Basin	35.239	79.300	1.45	1.40	1.53	1.46
sub-51	Above Ramganga Confluence Sub Basin	29.739	78.871	2.29	1.37	1.38	1.68
sub-52	Banas Sub Basin	25.944	75.096	1.15	1.35	1.41	1.30
sub-53	Bhagirathi and others (Ganga Lower) Sub Basin	24.199	87.973	1.38	1.47	1.40	1.41
sub-54	Chambal Lower Sub Basin	25.880	77.387	1.50	1.47	1.51	1.49
sub-55	Chambal Upper Sub Basin	23.728	75.444	1.39	1.41	1.46	1.42
sub-56	Damodar Sub Basin	23.268	86.650	1.37	1.47	1.38	1.41
sub-57	Gandak and others Sub Basin	25.440	85.408	1.47	1.54	1.56	1.52
sub-58	Ghaghara Confluence to Gomti confluence Sub Basin	25.587	83.455	1.39	1.41	1.45	1.42
sub-59	Ghaghara Sub Basin	27.654	82.074	1.49	1.37	1.48	1.45
sub-60	Gomti Sub Basin	26.802	81.171	1.40	1.41	1.46	1.42
sub-61	Kali Sindh and others up to Confluence with Parbati Sub Basin	24.450	76.437	1.74	1.79	1.94	1.82
sub-62	Ramganga Sub Basin	28.832	79.322	1.39	1.41	1.46	1.42
sub-63	Sone Sub Basin	23.793	82.595	1.47	1.53	1.55	1.52
sub-64	Tons Sub Basin	24.730	81.554	1.46	1.46	1.49	1.47
sub-65	Upstream of Gomti confluece to Muzaffarnagar Sub Basin	26.833	80.180	1.40	1.42	1.46	1.42
sub-66	Yamuna Lower Sub Basin	25.124	79.044	2.14	1.79	1.93	1.95
sub-67	Yamuna Middle Sub Basin	27.351	77.338	1.41	1.42	1.47	1.43
sub-68	Yamuna Upper Sub Basin	29.555	77.271	1.46	1.42	1.47	1.45
sub-69	Brahmaputra Lower Sub Basin	26.530	91.342	1.31	1.32	1.33	1.32
sub-70	Brahmaputra Upper Sub Basin	27.699	94.913	1.31	1.29	1.34	1.32
sub-71	Barak Sub Basin	24.486	93.026	1.41	1.43	1.46	1.43
sub-72	Kynchiang and other south flowing rivers Sub Basin	25.380	91.164	1.37	1.40	1.43	1.40
sub-73	Naoch chara and others Sub Basin	23.816	91.739	1.36	1.37	1.40	1.38
sub-74	Muhury and Others Sub Basin	23.218	91.572	1.33	1.34	1.38	1.35
sub-75	Godavari Lower Sub Basin	18.017	81.543	1.38	1.41	1.45	1.41

Table 2 (*continued*)

| Subbasin	Name of River (sub basin)	Latitude	Longitude	2003–2007	2008–2012	2013–2017	Fitted (2003–2017)
				$\omega 1$	$\omega 2$	$\omega 3$	$\omega 4$
sub-76	Godavari Middle Sub Basin	19.414	76.471	1.37	1.39	1.44	1.40
sub-77	Godavari Upper Sub Basin	19.744	74.485	1.40	1.41	1.44	1.41
sub-78	Indravati Sub Basin	19.448	81.350	1.37	1.39	1.44	1.40
sub-79	Manjra Sub Basin	18.226	77.199	1.40	1.41	1.45	1.42
sub-80	Pranhita and others Sub Basin	18.790	79.211	1.40	1.42	1.46	1.42
sub-81	Wardha Sub Basin	20.305	78.167	1.38	1.41	1.45	1.41
sub-82	Weinganga Sub Basin	21.348	79.680	1.39	1.41	1.45	1.42
sub-83	Bhima Lower Sub Basin	17.249	76.747	1.39	1.41	1.44	1.41
sub-84	Bhima Upper Sub Basin	18.207	74.813	1.37	1.39	1.44	1.40
sub-85	Krishna Lower Sub Basin	17.085	79.657	1.40	1.42	1.46	1.42
sub-86	Krishna Middle Sub Basin	16.462	78.261	1.38	1.40	1.43	1.40
sub-87	Krishna Upper Sub Basin	16.482	75.052	1.39	1.42	1.45	1.42
sub-88	Tungabhadra Lower Sub Basin	14.878	76.861	1.39	1.42	1.45	1.42
sub-89	Tungabhadra Upper Sub Basin	14.447	75.675	1.38	1.41	1.44	1.41
sub-90	Cauvery Lower Sub Basin	10.895	79.041	1.38	1.40	1.44	1.41
sub-91	Cauvery Middle Sub Basin	11.816	77.247	1.38	1.40	1.44	1.41
sub-92	Cauvery Upper Sub Basin	12.672	76.063	1.39	1.41	1.44	1.41
sub-93	Subarnarekha Sub Basin	22.411	86.295	1.38	1.40	1.44	1.41
sub-94	Baitarni Sub Basin	21.484	86.058	1.38	1.41	1.44	1.41
sub-95	Brahmani Sub Basin	21.969	85.054	1.39	1.41	1.44	1.41
sub-96	Mahanadi Lower Sub Basin	20.438	84.105	1.37	1.40	1.44	1.41
sub-97	Mahanadi Middle Sub Basin	21.833	82.920	1.37	1.40	1.44	1.40
sub-98	Mahanadi Upper Sub Basin	21.603	81.496	1.38	1.40	1.44	1.41
sub-99	Pennar Lower Sub Basin	14.345	79.092	1.38	1.41	1.44	1.41
sub-100	Pennar Upper Sub Basin	14.498	77.964	1.38	1.40	1.43	1.41
sub-101	Kosi Sub Basin	26.119	86.358	1.38	1.40	1.44	1.41
sub-102	Bhatsol and others Sub Basin	19.755	73.223	1.38	1.40	1.43	1.40
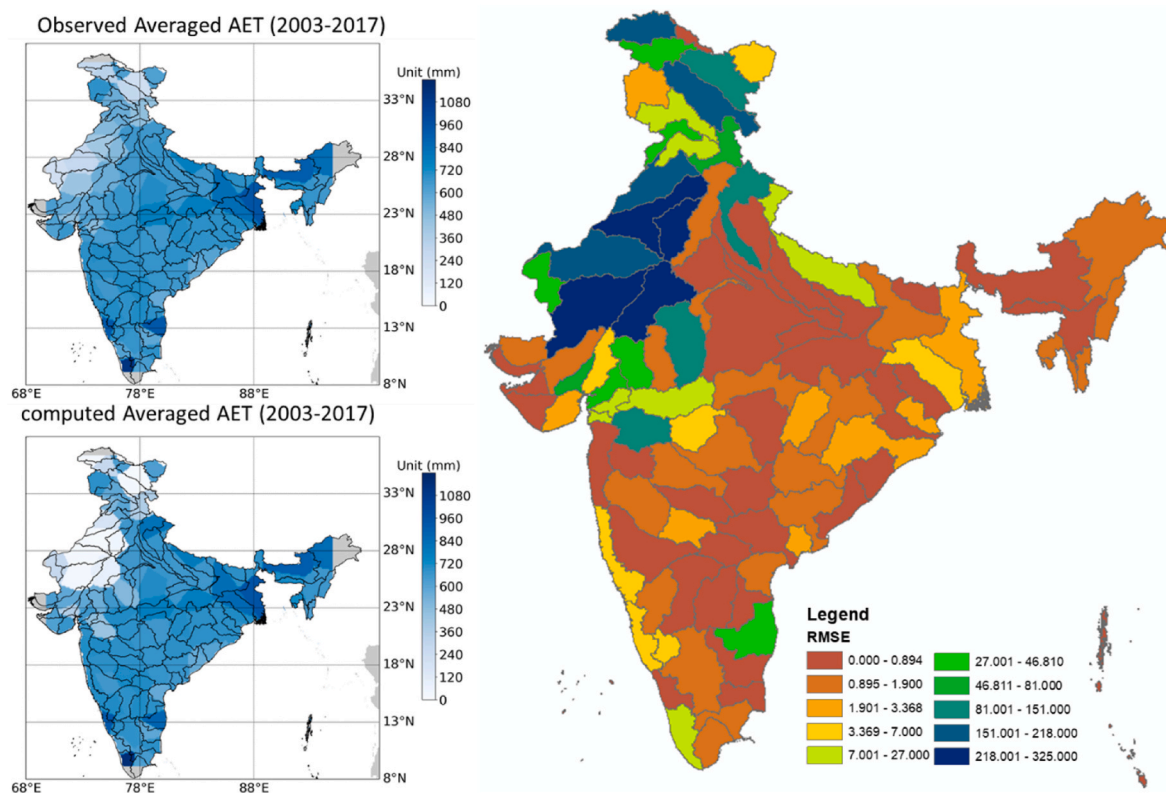
Fig. 12. Comparison between observed and simulated AET computed by the optimized "ω" parameter across each sub-basin by using Fu's Budyko equation in the average duration (2013–2017) (a, b) and (c) validation of optimized "ω" parameter across each sub-basin by Fu's Budyko equation in the average duration (2013–2017) by calculating RMSE between observed and "ω" based calculated AET.

many sub-basins (mostly SI. no. 1 to 20; i.e., the sub-basins of the Indus, Narmada and Tapi sub-basins) as compared to the other sub-basins of the Ganga, Godavari, Krishna and Cauvery and Mahanadi sub-basins. In another way, it can be also stated that most of the river sub-basins, parts of Northern India, Southern and Eastern India correspond to high responsivity than the sub-basins falling in the other parts of the country. The study finds that many river sub-basins (e.g. 1–9, 11–15, 17, 27, 35, 49–50, 66–67) correspond to ET-Blue and out of these, the sub-basins

2–4, 15, 27, 35, correspond to higher ET-Blue values than the other sub-basins. This shows that these sub-basins receive water from external sources like canal water supply or diversion from another basin to fulfil their evaporative water demand. These sub-basins should be on the priority side for agricultural water management through application of the advanced irrigation systems and increasing irrigation water use efficiency. These findings suggest that the increase in ET-Blue within the sub-basins may affect the overall water availability and enhance the water scarcity in case of increasing DI. If this persists so, then it may be stated that many of these sub-basins may be critical in fulfilling the evaporative water demands and face water scarcity conditions due to reduction in the amount of precipitation and high evaporative water demand. This study also finds that around ~50–60% of the water from precipitation turns into ET-Green in India and a significant variation in ET-Green will directly affect the rain-fed crop production and the corresponding area's water availability. The sub-basin wise spatial distribution of ET-Green, ET-Blue (demand side) and water yield (water availability) shows that ET-Green in sub-basins vary from ~50 mm to 1000 mm, whereas ET-Blue varied from ~5 mm to 260 mm. The maximum ET-Green (in mm) corresponded mostly to moderate to high rainfall areas like North-Eastern States part of Brahmaputra basin (e.g. river sub-basins such 69–70) and western Ghats (e.g. river sub-basins 27–29), whereas Jammu and Kashmir, Himachal Pradesh, several areas of the desert region (e.g. Rajasthan, Gujarat) and few areas of Southern India recorded low ET-Green (e.g. river sub-basins 2–17). Based on the spatial distribution of ET-Green, ET-Blue and water yield, it is found that the river sub-basins (e.g., 2, 4, 7–15, 24, 25, 52 and 66) are correspond to insufficient water yield. The results show that ET-Blue sub-basins will have more water demand than ET-Green sub-basins, where Precipitation is not sufficient to fulfil the demand and it depends an additional sources of water. There is enormous scope of the future research based on this work that the parameterized Fu's Budyko model, which is specific to each river sub-basin, will be of immense helpful to adopt sub-basin specific agricultural water management strategies, based on the ET-Green and ET-Blue estimates. Further, sub-basin specific parameterized Fu's Budyko model will be helpful in projecting future evaporative water demand, if either P or ET is known. Here it is worth mentioning that larger the availability of the AET station data better will be the results of estimation of evaporative water demand, partitioning of ET into ET-green and ET-blue and water availability estimates.

Conflict of interest

Authors report no conflict of interest for this research article.

CRediT authorship contribution statement

Vishal Singh: Conceptualization, Methodology, Software, Analysis, Writing – original draft, preparation. **Pushpendra Kumar Singh:** Conceptualization, Methodology, Writing – review & editing. **Sanjay Kumar Jain:** Visualization, Reviewing and Editing. **Sharad Kumar Jain:** Conceptualization, Investigation, Writing – review & editing. **Christophe Cudennec:** Writing – review & editing. **Tim Hessels:** Software, Methodology, Editing.

Declaration of competing interest

The authors declare that they have no known competing financial interests or personal relationships that could have appeared to influence the work reported in this paper.

Acknowledgement

Authors are kindly thankful to the National Institute of Hydrology Roorkee India for providing all facilities to carry out this research work.

References

Ambika, A.K., Wardlow, B., Mishra, V., 2016. Remotely sensed high resolution irrigated area mapping in India for 2000 to 2015. Sci. Data 3, 160118.

Bai, P., Liu, X., Zhang, D., Liu, C., 2020. Estimation of the Budyko model parameter for small basins in China. Hydrol. Proced. 34 (1), 125–138.

Budyko, M.I., Miller, D.H., Miller, D.H., 1974. Climate and Life, 508, New York. Academic press, USA.

Byrne, M.P., O'Gorman, P.A., 2015. The response of precipitation minus evapotranspiration to climate warming: why the "wet-get-wetter, dry-get-drier" scaling does not hold over land. J. Clim. 28 (20), 8078–8092.

Cao, G., Han, D., Song, X., 2014. Evaluating actual evapotranspiration and impacts of groundwater storage change in the North China Plain. Hydrol. Proced. 28 (4), 1797–1808.

Creed, I.F., Spargo, A.T., Jones, J.A., Buttle, J.M., Adams, M.B., Beall, F.D., Booth, E.G., Campbell, J.L., Clow, D., Elder, K., Green, M.B., 2014. Changing forest water yields in response to climate warming: results from long-term experimental watershed sites across North America. Global Change Biol. 20 (10), 3191–3208.

Fu, J., Wang, W., 2019. On the lower bound of Budyko curve: the influence of precipitation seasonality. J. Hydrol. 570, 292–303.

Goroshi, S., Pradhan, R., Singh, R.P., Singh, K.K., Parihar, J.S., 2017. Trend analysis of evapotranspiration over India: observed from long-term satellite measurements. J. Earth Syst. Sci. 126 (8), 113.

Greve, P., Gudmundsson, L., Orlowsky, B., Seneviratne, S.I., 2015. The Budyko framework beyond stationarity. Hydrol. Earth Syst. Sci. Discuss. 12 (7).

Gudmundsson, L., Greve, P., Seneviratne, S.I., 2016. The sensitivity of water availability to changes in the aridity index and other factors—a probabilistic analysis in the Budyko space. Geophys. Res. Lett. 43 (13), 6985–6994.

Gunkel, A., Lange, J., 2017. Water scarcity, data scarcity and the Budyko curve—an application in the Lower Jordan River Basin. J. Hydrol.: Reg. Stud. 12, 136–149.

Gupta, V., Jain, M.K., Singh, P.K., Singh, V., 2019. An assessment of global satellite-based precipitation datasets in capturing precipitation extremes: a comparison with observed precipitation dataset of India. Int. J. Climatol. 40 (8), 3667–3688. https://doi.org/10.1002/joc.6419.

Helman, D., Lensky, I.M., Yakir, D., Osem, Y., 2017. Forests growing under dry conditions have higher hydrological resilience to drought than do more humid forests. Global Change Biol. 23 (7), 2801–2817.

Huo, J., Liu, C., Yu, X., Jia, G., Chen, L., 2021. Effects of watershed char and climate variables on annual runoff in different climatic zones in China. Sci. Total Environ. 754, 142157.

India-Wris, 2012. River Basin Atlas of India. RRSC-West, NRSC, ISRO, Jodhpur, India. https://indiawris.gov.in/downloads/RiverBasinAtlas_Full.pdf.

Jha, S., Das, J., Sharma, A., Hazra, B., Goyal, M.K., 2019. Probabilistic evaluation of vegetation drought likelihood and its implications to resilience across India. Global Planet. Change 176, 23–35.

Jhajharia, D., Shrivastava, S.K., Sarkar, D.S.A.S., Sarkar, S., 2009. Temporal characteristics of pan evaporation trends under the humid conditions of northeast India. Agric. For. Meteorol. 149 (5), 763–770.

Joseph, J., Ghosh, S., Pathak, A., Sahai, A.K., 2018. Hydrologic impacts of climate change: comparisons between hydrological parameter uncertainty and climate model uncertainty. J. Hydrol. 566, 1–22.

Katyaini, S., Barua, A., Duarte, R., 2020. Science-policy interface on water scarcity in India: giving 'visibility' to unsustainable virtual water flows (1996–2014). J. Clean. Prod. 275, 124059. https://doi.org/10.1016/j.jclepro.2020.124059.

Khan, M.S., Liaqat, U.W., Baik, J., Choi, M., 2018. Stand-alone uncertainty characterization of GLEAM, GLDAS and MOD16 evapotranspiration products using an extended triple collocation approach. Agric. For. Meteorol. 252, 256–268.

Kundu, S., Khare, D., Mondal, A., 2017. Interrelationship of rainfall, temperature and reference evapotranspiration trends and their net response to the climate change in Central India. Theor. Appl. Climatol. 130 (3–4), 879–900.

Kundu, S., Mondal, A., Khare, D., Hain, C., Lakshmi, V., 2018. Projecting climate and land use change impacts on actual evapotranspiration for the Narmada river basin in Central India in the future. Rem. Sens. 10 (4), 578.

Lahiri, I., 2019. Promoting Rural Development in Border Disturbed Regions of India through Inclusive Growth in Agriculture by Using Open and Distance Learning Technologies (ODL).

Li, Y., Liu, C., Yu, W., Tian, D., Bai, P., 2019. Response of streamflow to environmental changes: a Budyko-type analysis based on 144 river basins over China. Sci. Total Environ. 664, 824–833.

Li, J., Zhang, C., Zhu, S., 2021. Relative contributions of climate and land-use change to ecosystem services in arid inland basins. J. Clean. Prod. 298, 126844. https://doi.org/10.1016/j.jclepro.2021.126844.

Liu, J., Xu, S., Han, X., Chen, X., He, R., 2019. A multi-dimensional hydro-climatic similarity and classification framework based on Budyko theory for continental-scale Applications in China. Water 11 (2), 319.

Lyon, S.W., King, K., Polpanich, O.U., Lacombe, G., 2017. Assessing hydrologic changes across the lower mekong basin. J. Hydrol.: Reg. Stud. 12, 303–314.

McMillan, H., Montanari, A., Cudennec, C., Savenije, H., Kreibich, H., Krueger, T., Liu, J., Mejia, A., Van Loon, A., Aksoy, H., Di Baldassarre, G., 2016. Panta Rhei 2013–2015: global perspectives on hydrology, society and change. Hydrol. Sci. J. 61 (7), 1174–1191.

Pal, L., Ojha, C.S.P., Kumar, A., 2021. Characteristics of GLDAS evapotranspiration and its response to climate variability across Ganga basin, India. Climate Change Impacts on Water Resources: Hydraulics, Water Res. Coastal Eng. 241–251.

Park, J., Choi, M., 2015. Estimation of evapotranspiration from ground-based meteorological data and global land data assimilation system (GLDAS). Stoch. Environ. Res. Risk Assess. 29 (8), 1963–1992.

Paulo, A.A., Rosa, R.D., Pereira, L.S., 2012. Climate trends and behaviour of drought indices based on precipitation and evapotranspiration in Portugal. Nat. Hazards Earth Syst. Sci. 12 (5), 1481–1491.

Pingale, S.M., Khare, D., Jat, M.K., Adamowski, J., 2016. Trend analysis of climatic variables in an arid and semi-arid region of the Ajmer District, Rajasthan, India. J. Water Land Dev. 28 (1), 3–18.

Poonia, V., Das, J., Goyal, M.K., 2021. Impact of climate change on crop water and irrigation requirements over eastern Himalayan region. Stoch. Environ. Res. Risk Assess. 35 (6), 1175–1188.

Ramarao, M.V.S., Sanjay, J., Krishnan, R., Mujumdar, M., Bazaz, A., Revi, A., 2019. On observed aridity changes over the semiarid regions of India in a warming climate. Theor. Appl. Climatol. 136 (1), 693–702.

Schmidt, J., Kienzle, S.W., Srinivasan, M.S., 2009. Estimating increased evapotranspiration losses caused by irrigated agriculture as part of the water balance of the Orari Catchment, Canterbury, New Zealand. J. Hydrol. 48 (2), 73–94.

Shrestha, M., Acharya, S.C., Shrestha, P.K., 2017. Bias correction of climate models for hydrological modelling–are simple methods still useful? Meteorol. Appl. 24 (3), 531–539.

Simons, G.W.H., Bastiaanssen, W.G.M., Cheema, M.J.M., Ahmad, B., Immerzeel, W.W., 2020. A novel method to quantify consumed fractions and non-consumptive use of irrigation water: application to the indus Basin irrigation system of Pakistan. Agric. Water Manag. 236, 106174.

Singh, A., Krause, P., Panda, S.N., Flugel, W.A., 2010. Rising water table: a threat to sustainable agriculture in an irrigated semi-arid region of Haryana, India. Agric. Water Manag. 97 (10), 1443–1451.

Singh, P.K., Jain, S.K., Mishra, P.K., Goel, M.K., 2021. An assessment of water consumption patterns and land productivity and water productivity using WA+ framework and satellite data inputs. Phys. Chem. Earth, Parts A/B/C 103053. https://doi.org/10.1016/j.pce.2021.103053.

Singh, R., Kumar, R., 2015. Vulnerability of water availability in India due to climate change: a bottom-up probabilistic Budyko analysis. Geophys. Res. Lett. 42 (22), 9799–9807.

Singh, R., Kumar, R., 2019. Climate versus demographic controls on water availability across India at 1.5° C, 2.0° C and 3.0° C global warming levels. Global Planet. Change 177, 1–9.

Singh, V., Xiaosheng, Q., 2019a. Study of rainfall variabilities in Southeast Asia using long-term gridded rainfall and its substantiation through global climate indices. J. Hydrol. 124320 https://doi.org/10.1016/j.jhydrol.2019.124320.

Singh, V., Xiaosheng, Q., 2019b. Data assimilation for constructing long-term gridded daily rainfall time series over Southeast Asia. Clim. Dynam. 1–25 (53), 3289. https://doi.org/10.1007/s00382-019-04703-6.

Sinha, J., Sharma, A., Khan, M., Goyal, M.K., 2018. Assessment of the impacts of climatic variability and anthropogenic stress on hydrologic resilience to warming shifts in Peninsular India. Sci. Rep. 8 (1), 13833.

Smith, S., Lasdon, L., 1992. Solving large sparse nonlinear programs using GRG. ORSA J. Comput. 4 (1), 2–15.

Smilovic, M., Gleeson, T., Siebert, S., 2015. The limits of increasing food production with irrigation in India. Food Sec 7 (4), 835–856.

Sonali, P., Nagesh Kumar, D., 2016. Spatio-temporal variability of temperature and potential evapotranspiration over India. J. Wat. Clim. Chang. 7 (4), 810–822.

Soni, D.K., Singh, K.K., 2017. Trend analysis of climatic parameters at kurukshetra (Haryana), India and its influence on reference evapotranspiration. In: Garg, V., Singh, V., Raj, V. (Eds.), Development of Water Resources in India. Water Science and Technology Library, vol. 75. Springer, Cham. https://doi.org/10.1007/978-3-319-55125-8_28.

Sposito, G., 2017. Understanding the Budyko equation. Water 9 (4), 236. https://doi.org/10.3390/w9040236.

Surendran, U., Raja, P., Jayakumar, M., Ramasubramoniam, S., 2021. Use of Efficient Water Saving Techniques for Production of Rice in India under Climate Change Scenario: A Critical.

Yang, Z., Zhang, Q., Hao, X., 2016. Evapotranspiration trend and its relationship with precipitation over the loess plateau during the last three decades. Adv. Meteorol. 2016, 5984595 https://doi.org/10.1155/2016/6809749.

Zhan, S., Song, C., Wang, J., Sheng, Y., Quan, J., 2019. A global assessment of terrestrial evapotranspiration increase due to surface water area change. Earth's Future 7 (3), 266–282.